www.envsciarch.com

ENVIRONMENTAL SCIENCE ARCHIVES
ISSN: 2583-5092
Volume III Issue 2, 2024

RESEARCH PAPER OPEN ACCESS

One Pot Synthesized 2H - MoS2 as Efficient Photocatalyst for Degradation of Titan Yellow Dye under Solar Light Illumination

Ajay kumar[1], Manisha[1], Rekha Bhardwaj[2], Divya Deep Yadav[1,3], Anju[1] and Ranjana Jha[1]

[1]Research Lab for Energy Systems, Department of Physics, N.S.U.T, Dwarka, New Delhi-110078, India
[2]Department of Applied Sciences, Bharati Vidyapeeth College of Engineering, New Delhi-110063, India
[3]Ramjas College, University Enclave, University of Delhi, Delhi-110007, India
Correspondence for materials should be addressed to AK (email: ajay211193@gmail.com)

Received: 2024/08/18
Accepted: 2024/09/23
Published: 2024/10/02

Abstract

Molybdenum disulfide (MoS2) was synthesized and employed as a promising catalyst under sunlight illumination for the photocatalytic degradation of Titan yellow (TY) dye. The structural and physiochemical features of the hydrothermally synthesized MoS2 nanoparticles were examined by X-ray Diffraction (XRD), X-ray Photoelectron Spectroscopy (XPS), Field Emission Scanning Electron Microscopy (FESEM), High-Resolution Transmission Electron Microscopy (HR-TEM) and UV-Vis spectrophotometer. XRD affirmed the formation of 2H-MoS2, which is the most stable phase of the MoS2. Additionally, morphological insights into the MoS2 nanospheres were obtained through Field Emission Scanning Electron Microscopy (FESEM). The photodegradation process and energy band gap value were analyzed using UV-visible absorption spectroscopy. Due to visible light responsive band gap of synthesized MoS2, it showed excellent degradation efficiency of 96 % under natural sunlight in a small-time duration (12 minutes). All the characteristics features of this study anticipated that MoS2 can be used as potential photocatalyst for cleaning our river, water treatment and environmental remediation.

Keywords: Nanosphere; Photocatalyst; 2H phase; Waste water treatment; Titan yellow Dye

Introduction

Due to the expansion of industrialization and climatic variations caused the decline of environmental health and the shortage of renewable energy sources. Our Industrial effluents and agriculture waste decreases the oxygen level of water which is the great threat of aquatic ecosystem. Water bodies are affected by the disposal of industrial waste into rivers, and a significant problem is created when industrial effluents are not purified. Contamination of drinking water is a serious issue that requires vigilant attention. Rising populations mean more pure water required for our society. Different types of pollutants like pharmaceuticals produces antibiotics, organic dye, polycyclic aromatic hydrocarbons, pathogenic microorganism, etc. are the major contaminants which are challenging to disintegrate entirely. There are numerous industries that releases harmful dye pollutants and other waste materials like leather, food, rubber, pesticide, etc. into water streams .These pollutants which are emitted into our food chain and environment through industry and agriculture waste are carcinogenic and mutagenic (Dutta et al., 2024; Lanjwani et al., 2024; Lin et al., 2023; Kumari et al., 2023).

Therefore, early detection and reliable degradation of toxic organic compounds, heavy metal ions, pesticides, etc., from water bodies and environment are urgently insistent. In order to improve the deteriorating condition of our environment, different types of microbiological and physicochemical techniques like adsorption, sedimentations, flocculations, coagulations, etc. were exercised over the past few years. Out of these techniques photocatalysis is the commonly employed for water

purification, due to its ease of acquisition and accessibility while performing this technique (Agasti 2021; Al-Tohamy et al., 2022).

The photocatalytic degradation process is one of the rapidly expanding technologies for the efficient degradation of organic pollutants. Semiconductor based metal oxide photocatalyst like ZrO_2, CeO_2, ZnO, SnO_2, TiO_2, WO_3, Co_3O_4, CuO, Cu_2O, and NiO, have been utilized. Because of their properties, such as photon absorption capacity, stability, non-toxicity, high activity, and high surface area, these semiconductor photocatalysts have been the subject of extensive research. However, there are several limitations of metal oxides, they possess broad bandgap which falls in the ultraviolet (UV) region which make researchers to seek alternatives of metal oxides. Efficiency of photocatalyst depends upon the surface area of the nanostructures which are used as photocatalyst. Due to immense surface area and tunable energy band gap of heterogeneous transition metal sulfide/oxide such as Cu_2O, TiO_2, ZnO, CdS, BN, ZnS, and ZrO_2 were used as photocatalysts (Sultana et al., 2023; Ashpak Shaikh et al., 2023; Pascariu et al.,2023; Gautam et al.,2020; Nemiwal et al., 2021; Nur et al., 2022; Yadav et al.,2022).

The layered transition metal dichalcogenides (LTMD) are one of type of nanomaterial that has garnered the attention of researcher. The energy bandgap of these 2D IV-VI semiconductor nanomaterials lies in the visible spectrum, and their high surface-to-volume ratio makes them promising adsorption sites for organic molecules. Over the last few years, many researchers in the field of material chemistry and microbiology are focusing to develop a novel photocatalysts that are cost-effective and highly efficient. MoS_2 attracts more attention as a photocatalysts due to their unique features such as tunable band gap, visible light absorption capacity, good electrical carrier mobility, high chemical reactivity, and high specific surface area. 2-D layered nanostructures molybdenum disulfide (MoS_2) has demonstrated excellent capacity for visible-light driven in photocatalytic applications (Sahoo et al., 2022; Shinde et al., 2023; Singh et al., 2020). MoS_2 has a trigonal prismatic structure, with Mo and S atoms connect strongly via covalent bonding between each layer. Mo atomic layer is located between two S atomic layers, each of which is hexagonal in shape. Owing to the weak Van der Waals interactions between the Mo and S, that assist in the stacking of MoS_2 layers, it has been shown that monolayer MoS_2 produced from micro-mechanical cleavage due to the fragile hydrogen bonds in the interlayer bonding. Yet, it is still difficult to obtain a high yield of MoS_2 monolayers via microexfoliation.

Due to lack of spatial inversion symmetry and strong d-orbital coupling MoS_2 shows the indirect to direct transition due to this it shows both direct and indirect energy band gap semiconductor. MoS_2 possesses an indirect bandgap of approximately 1.3 eV in its bulk state and transitions to a direct bandgap of about 1.9 eV when reduced to a single-layer form. Due to direct to indirect transition it has many applications in various field, because of its high yield and good quality (Ji et al., 2022; Kumar et al., 2019; Sahoo et al., 2020); Yuan et al., 2021).

In this paper, 2H-MoS_2 nanosheet were synthesized by a simple hydrothermal method. Various Structural and physiochemical features of the hydrothermally synthesized MoS_2 was examined through various technique. MoS_2 used as photocatalyst for degradation of Titan yellow dye. MoS_2 photocatalyst further used as river purification and environmental sustainability.

Experimental detail

Chemicals used

Sodium molybdate ($Na_2MoO_4{\cdot}2H_2O$), Thiourea (CH_4N_2S), were brought from Sigma-Aldrich Co. Ltd. Oxalic acid and Titan yellow dye were purchased from loba chemie. All the reagents were of analytical grade and used for the synthesis of MoS_2 nanoparticles without purification.

Synthesis method

MoS_2 nanoparticles was synthesized by hydrothermal technique. In 100 ml of Millipore water, 0.2 mol of sodium molybdate and 0.4 mol of Thiourea were introduced with continuous stirring for 3 hours. Then, 0.1 mol of oxalic acid was added while stirring, which was acted as reducing agent. The resultant solution was moved into autoclave with Teflon lined and kept in a hot air oven at 200 °C for 20 hours, after naturally cooled down, autoclave was removed from the hot air oven and final product was filtered by centrifugation technique. Obtained precipitate was washed from Millipore water and ethanol three times. Finally, product was kept in a vacuum oven at 60°C for 15 hours to remove excess of water and moisture. Black color powder was ground for 1 hours and end product was acquired.

Characterization of grown MoS_2 nanostructures

Crystal rotating High -Resolution X-ray Diffractometer (HR-XRD, Bruker D8 Discover) technique was conducted to study the phase, structure, crystallographic structure and composition of the materials. Morphology of the nanoparticles were investigated by Field emission scanning electron microscope (FESEM, Zeiss Gemini SEM 500) and High-Resolution transmission electron microscope (HRTEM, JEOL JEM 2100 PLUS). Electronic state of the prepared nanoparticles was studied by X-Ray Photoelectron Spectroscopy (XPS, Thermo Fisher Model-K Alpha). UV-vis diffuse reflectance spectroscopy (DRS, Shimadzu UV-2600i Spectrometer) was exercised to analyze the forbidden energy band gap and photocatalytic activity of the nanoparticles. To evaluate the pore size and their distribution was exercised through Brunauer-Emmett-Teller (BET, NOVA 2200e) technique. Vibrational band of the dye and degraded product was study by Fourier Transform Infrared Spectroscopy (FTIR, Perkin Elmer).

Results and discussions

XRD Analysis

Figure 1(a) demonstrates the XRD plot of the MoS_2 nanoparticles showing diffraction peaks at 13.7°, 33.1°, and 58.7°, which are equivalent to the (002), (101), and (110) planes. These peaks confirm the presence of a hexagonal (2H) phase structure. The prominent peak at 13.7° (002 plane) verifies the establishment of the 2H phase of MoS_2. Additionally, the peaks at 33.1° (101 plane) and 58.7° (110 plane) further validate the pure phase of the MoS_2 structure, as no impurity peaks are detected. The lattice spacing is determined using the formula provided below, yielding a value of 0.66 nm (Nayak et al., 2023)

$$2\,d\,sin\,\theta = n\lambda \qquad (1)$$

The crystallite size (D) is determined using the Debye-Scherrer equation, as shown below

$$D = \frac{k\lambda}{\beta_{hkl} cos\theta} \qquad (2)$$

In this context, k is the shape factor (0.9), λ signifies the X-ray source wavelength, β indicates the full width at half-maximum (FWHM), and θ is Bragg's diffraction angle. The crystallite size was found to be 0.95 nm (at 2θ =13.7°). The Williamson-Hall (W-H) plot considers strain, enabling more accurate determinations of crystallite size and strain. The W-H plots was plotted, as shown in figure 1(b), using the Williamson-Hall equation, presented in the following equation (Dipti et al., 2023)

$$B cos\theta = \varepsilon(4sin\theta) + \frac{K\lambda}{D} \qquad (3)$$

In this equation, D indicates the crystallite size, K symbolizes Scherer's constant (0.9), λ signifies the wavelength of the Cu source, β represents the Full Width at Half Maximum (FWHM), θ denotes the peak position, and ε stands for strain. The slope values are determined as 0.05441, using linear fitting indicates the strain present in the material. Crystallite size determined by equation (2) is 0.70nm.

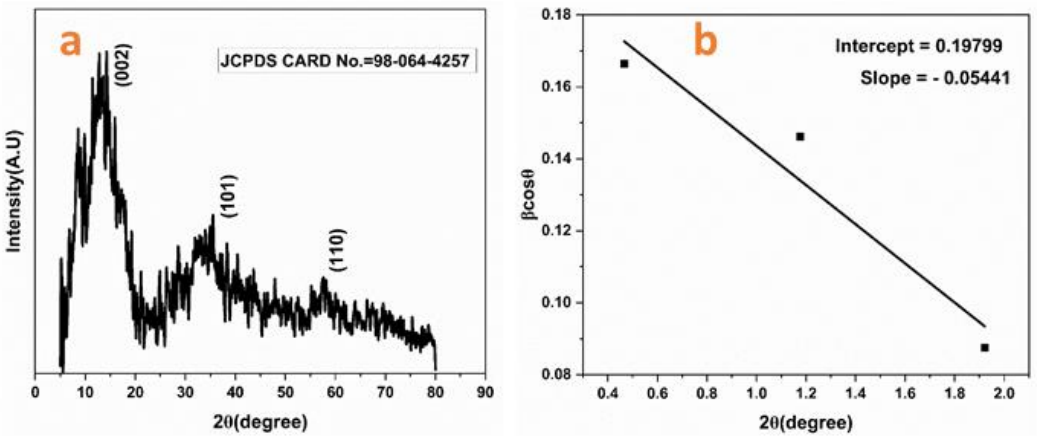

Fig.1 (a,b) XRD plot of synthesized MoS_2 nanosphere and W-H plot

FESEM Analysis

FESEM images were captured at resolutions ranging from 2 µm to 200 nm for the prepared sample, revealing morphology of MoS_2 as nanosheet with some nanorods (figure 2 a,b). The surface

structure is vital for applications in photocatalysis. Both the morphology plays a vital role in the photocatalytic activity because 1-D nano rods provide the direct pathway for migration of dye molecules into photocatalyst active site for photocatalyst degradation. Nanosheet possesses a substantial surface area, attributed to the abundance of active sites available for photodegradation. The nanosheet with some nanorods, morphology of MoS_2 is effective in degrading titan yellow dye because its large surface area and high porosity enhance its performance.

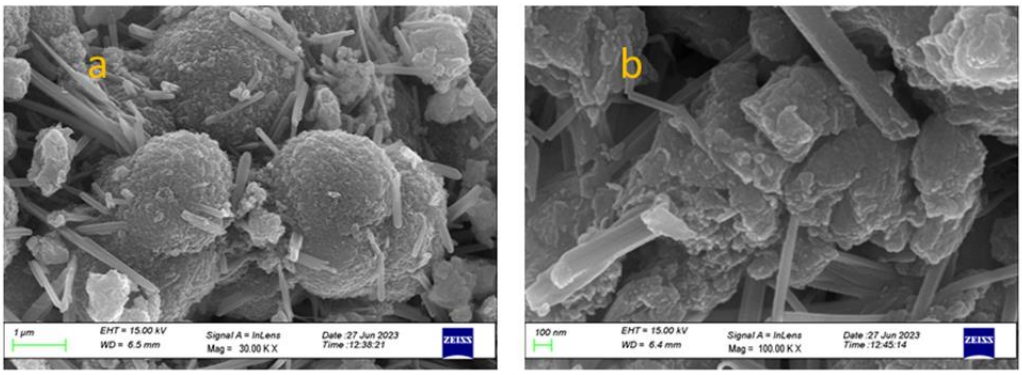

Fig.2(a, b). FESEM image of prepared sample of MoS_2

HRTEM Analysis

HRTEM images were captured using a 300-mesh copper grid to obtain highly magnified views of the prepared sample (figure 3). TEM image of the synthesized sample observed at resolutions of 50 and 5 nm (figure 3 a,b). Using Image J software, the interplanar spacing or line spacing of the prepared MoS_2 nanoparticles was calculated and its value is 0.67 nm which is approximately match to XRD data which discussed in section 3.1.

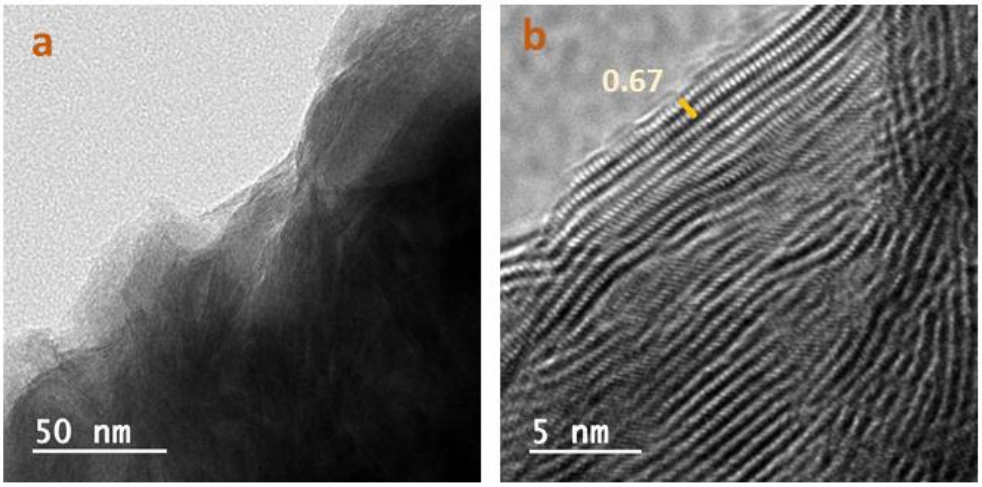

Fig.3 (a, b) HRTEM image of prepared sample of MoS_2

XPS Analysis

XPS technique was employed to analyze the composition, oxidation, electronic and chemical states of prepared MoS_2.XPS survey display in figure4(a). Survey spectra of MoS_2 depicted the existence of C, Mo, S and C elements in the prepared MoS_2 nanoparticles. Mo 3d orbital spectrum is display in figure4 (b) reveals the binding energy of an orbital state Mo $3d_{3/2}$ and Mo $3d_{5/2}$ peaks at 231.7 eV and 228.3 eV, respectively. This binding energy of orbital states affirms the oxidation state of MoS_2 in Mo^{4+} state. In figure 4(c) represents the orbital spectra of S2p which having two p orbital peaks S $2p_{3/2}$ and S $2p_{1/2}$ and their corresponding binding energy is 161.1eV and 162.2 eV, respectively. Both peaks of S $2p_{3/2}$ and S $2p_{1/2}$ represents the dual oxidation state of Sulphur (Alhammadi et al., 2020).

UV -Visible spectroscopy

The electronic spectrum and optical properties of the synthesized MoS_2 nanospheres were thoroughly examined using DRS method-based UV-Visible spectroscopy within the 190–800 nm wavelength range. The UV-Vis reflectance spectrum for MoS_2 nanosheet is depicted in figure (5). The optical band gap (E_g) calculated for MoS_2 nanosheet using Kubelka-Munk function. The graph was plotted between $[F(R_\infty)hv]^{1/n}$ vs hv as shown in inset image in figure (5), the intercept of the plotted represents the accurate value of the energy band gap. MoS_2 is a direct band gap material

so, n=2. The energy band gap is calculated by the Kubelka- Munk model equation given by (Panchu et al., 2021)

$$\frac{k}{s} = \frac{(1-R_\infty)^2}{R_\infty} = F(R_\infty) \qquad (4)$$

Where F (R_∞) represents Kubelka-Munk function, R_∞ represents reflectance, s is scattering coefficient, and k is absorption. The energy band gap value was calculated to be 1.7 eV for MoS_2 nanosphere.

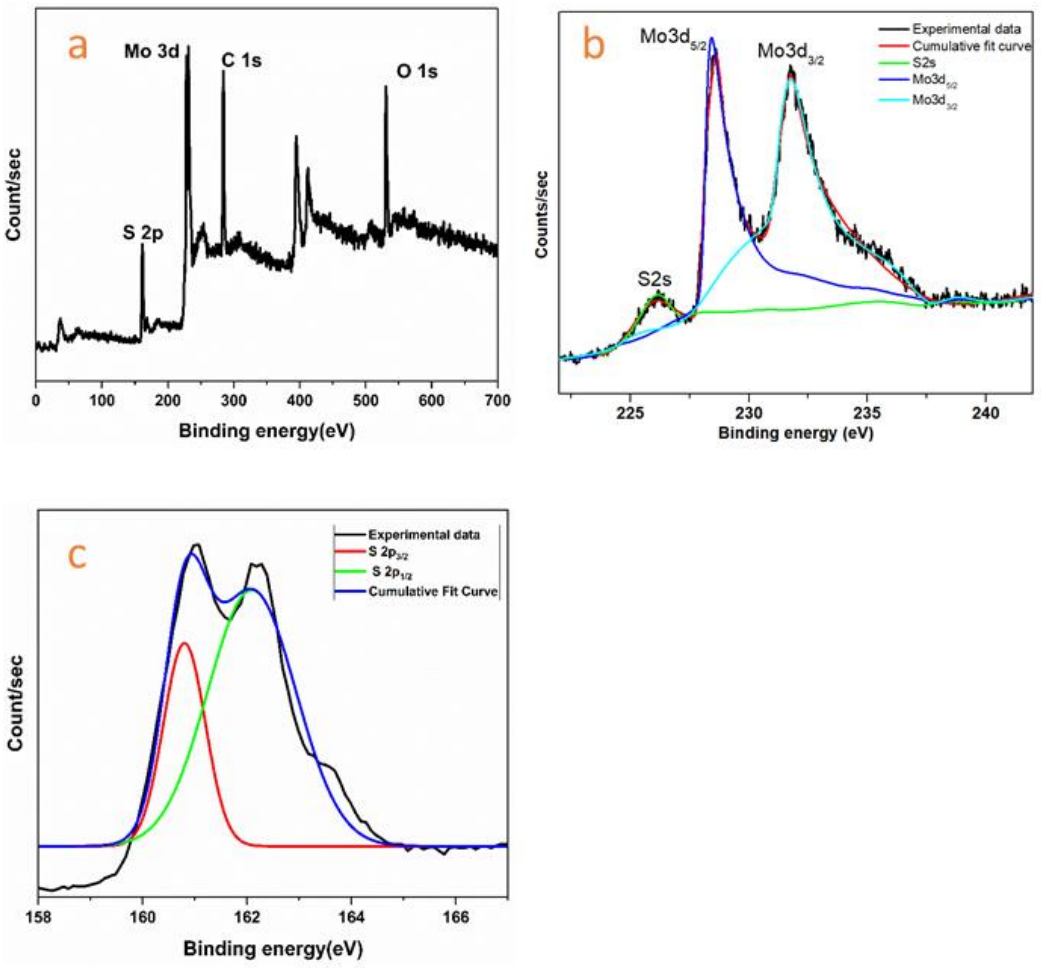

Figure.4 (a) XPS survey of MoS_2 nanosheet, (b) the XPS spectra of Mo 3d core level, and (c) the XPS spectra of S 2p for MoS_2

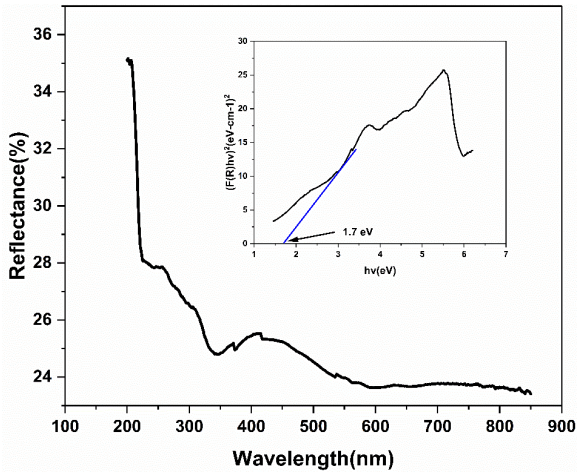

Fig.5. UV-Visible reflectance spectra of MoS_2 and inset image represent the K-M graph to evaluate energy band gap

BET

To investigate textural property of MoS_2 was analyzed by nitrogen adsorption-desorption isotherm. Hysteresis curve of the MoS_2 as display in figure 6(a), Hysteresis curve represents the type IV

isotherms which affirms the synthesized nanoparticles are porous in structure (Bhardwaj et al., 2020). Using Brunauer-Emmett-Teller (BET) technique from equation (5-8) surface area and pore size of the prepared sample were calculated. Surface area, pore size and pore volume of MoS_2 nanoparticles are 15.36m2/g, 3.8 nm and 0.05nm, respectively and respective graph are shown in figure6 (a,b,c).

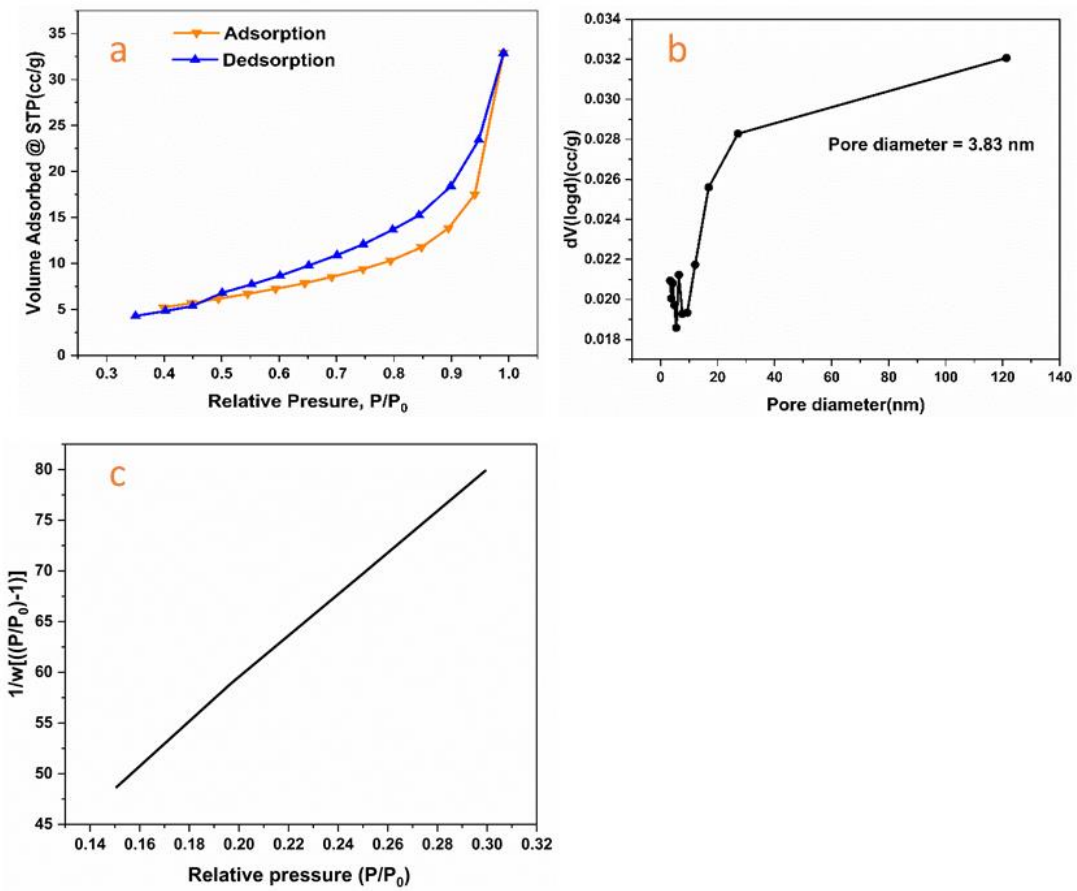

Fig.6. Nitrogen adsorption-desorption isotherms of MoS_2 nanosheet (b) Pore size distribution plot (c) BET plot of the MoS_2 nanosheet.

Due to large pore size, organic molecules can be easily adsorbed on the surface of nanoparticles and large surface provides more number active sites for photocatalytic dye degradation. All the characteristics shows that prepared MoS_2 nanoparticles used as efficient photocatalyst. Pore diameter, surface area, and pore volume were calculated using following equations:

$$\frac{1}{W\left[\frac{p_0}{p}-1\right]} = \frac{1}{W_m C} + \frac{C-1}{W_m C} \qquad (5)$$

Where w represents weight of gas absorbed, $\frac{p_0}{p}$ represents relative pressure, W_m is weight of adsorbate and C is BET constant. Above equation represents a linear equation where, $\frac{1}{W_m C}$ = i, represents the intercept and $\frac{C-1}{W_m C}$ = S, represents the slope of straight line

$$W_m = \frac{1}{i+S} \qquad (6)$$

Surface area was calculated utilizing following equation

$$S_t = \frac{N W_m A_{cs}}{M} \qquad (7)$$

Where N is Avogadro's number, S_t is total surface area, A_{cs} is adsorbate cross sectional area.

$$S_a = \frac{S_t}{W} \qquad (8)$$

S_a is specific area (P Bhardwaj R et al., 2020).

Photocatalytic Activity of MoS_2

The degradation of TY dye using MoS_2 nanosheet was tested under solar irradiation. Degradation has been observed using UV-visible absorption spectroscopy, which measures the decline in dye absorbance as a function of time. Nanosheet had their photocatalytic activity (PCA) measured by using a dye solution stored in the dark. To attain adsorption/desorption equilibrium place a 100 ml solution of the dye with 40 mg of MoS_2 nanosheets for 10 minutes in the dark environment. To further separate the bigger catalyst particles, around 10-15 mL of the mixture was removed and centrifuged at 7000 rpm for 2 minutes. Next, the adsorption/desorption isotherm was utilized to determine the degree to which the dye had degraded in the solution. A decrease in the UV peak at 405 nm indicates the degradation of the TY dye over time, as demonstrated in figure 7. Spectral absorption patterns of the dye solution and plot of concentration ratio (C/C_0) under solar irradiation with MoS_2 nanosheet are shown in the figure (7(a,b)). The absorbance of the dye gradually decreased over time when exposed to sunlight irradiation with MoS_2 NSs, indicating its degradation. Notably, the dye disappeared 96% after only 12 minutes. Table 2 presents an overview of the photocatalytic degradation of MoS_2-based materials. Dye degradation was measured as a percentage, using eq. (9) as a formula.

$$\text{Degradation Efficiency (\%)} = [(C_0\text{-}C)/C_0] \times 100\% \qquad (9)$$

where C_0 and C represent the absorbance values at zero light (or no light) and the desired light intensity (I). The rate constants involved in the degradation of TY dye by MoS_2 NS was calculated using Equation 10

$$\ln(C/C_0) = -kt \qquad (10)$$

which follows pseudo first order kinematics, where the time of exposure is denoted by t and the proportionality constant is denoted by k (RM et al., 2022; Rahman et al., 2020). The oxidation of the TY dye through photoactive MoS_2 nanosheet is a graph of ln(C/Co) against the exposure time (t) (figure7(c)), which is a good fit for a pseudo-first-order kinetic model. The rate constant was determined using mathematical analysis, model fitting results showed a slope of 0.25 min^{-1} which is illustrated in figure (7(c)). Under solar irradiation, the Photocatalytic analysis (PCA) of MoS_2 nanosheet on TY dye can be best explained by the process's underlying mechanism. Conduction band electrons in the catalyst react with oxygen atoms, releasing system, causing free radicals of the form superoxide ($\bullet O^{2-}$) to be produced. Then, the H^+ reacts with the radicals' ions to create H_2O_2, which then breaks down into •OH radicals. In addition, the excitonic electron-hole pair decays, leaving holes in the conduction band, create •OH radicals by reacting with water molecules in the solution. Dye adsorbed on the catalyst's surface interacts with the •OH radicals, releasing of CO_2 /H_2O in the environment (Hayashi T et al., 2020).

$$MoS_2\ NS + TY \xrightarrow[10\ min]{} \text{Dye adsorbed on } MoS_2 \text{ NSs}$$

$$MoS_2\ NSs \xrightarrow{\text{Solar irradiation}} MoS_2 \longrightarrow e^-\text{-}h^+ \text{ pair}$$

$$e^- + O_2 \longrightarrow {}^{\bullet}O_2^-$$

$$H_2O \longrightarrow H^+ + OH^-$$

$${}^{\bullet}O_2^- + H^+ \longrightarrow H_2O_2$$

$$H_2O_2 \longrightarrow {}^{\bullet}OH$$

$$h^+ + OH^- \longrightarrow {}^{\bullet}OH$$

$${}^{\bullet}OH + \text{TY dye} \longrightarrow CO_2/H_2O$$

The mechanism was verified using free radical trapping experiments which was done using benzo quinone, and methanol to trap O_2^-, h^+/·OH. As shown in figure (8). the photocatalytic activity was reduced to 65% in the presence of methanol, while it decreased to 83%, in the presence of benzoquinone. Based on these results, the h^+/· OH radical plays the major role in photocatalytic degradation of TY dye.

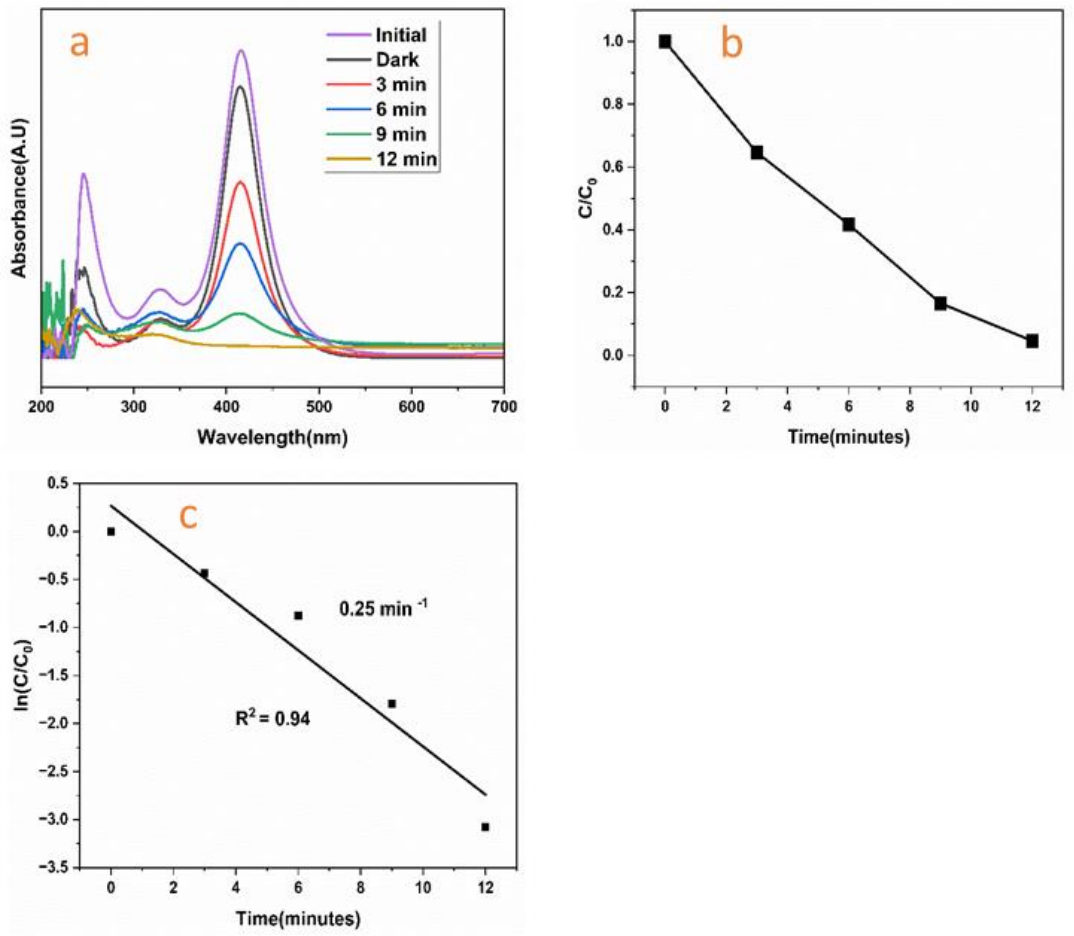

Fig.7 (a,b,c) Plot of absorption spectra, concentration ratio (C/Co) and ln (C/C_0)

FTIR analysis of Titan Yellow (TY) dye was carried out before and after the photocatalytic degradation to confirm the final product formation. The FT-IR spectra of titan yellow dye and reduced product are shown in figure 9 (a,b). The asymmetric stretching due to -CH_3 group was detected at peak 2924 cm^{-1} and an azo group of N = N stretching was observed at 1535 cm^{-1}. The peaks at 1739 cm^{-1} correspond to C=O stretch and peak at 1456 cm^{-1} correspond to -CH_3 bending vibration. The sulphonic nature(S=O) of azo dye was represented at peak value of 1365 cm^{-1} and 1215 cm^{-1}. The stretching vibration at 1100 cm^{-1} indicated -C-N which represented the azo nature of the dye. The peak at 535 cm^{-1} indicated –C–S– stretching vibrations.

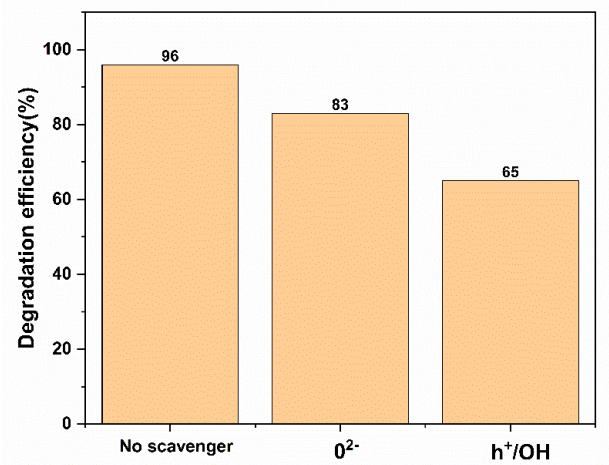

Fig.8. Effect of various scavengers on the degradation of TY dye.

After the addition of MoS_2 nanosheet, FTIR spectra of the reduced product of TY show an intensity broad distinct peak at 3305 cm^{-1} for –N–H stretching of amine and peak at 1638 cm^{-1} for –N–H bending vibrations; this confirms azo group reduction. Additionally, missing peaks for –N=N– stretching vibrations at 1535 cm^{-1} confirm the reduction of the azo group. The peak at 1215 cm^{-1} and

1365 cm^{-1} corresponding to –S=O stretching vibrations (confirm the presence of sulfonic group) and peak at 581 cm^{-1} for –C–S– stretching vibrations were present in the reduced product also (figure 9(b)). In the degraded sample, the missing peak indicated the group was eliminated during decolorization. Degraded products showed new peaks indicating that TY has been degraded by MoS_2 nanoparticle (Carolin et al., 2021).

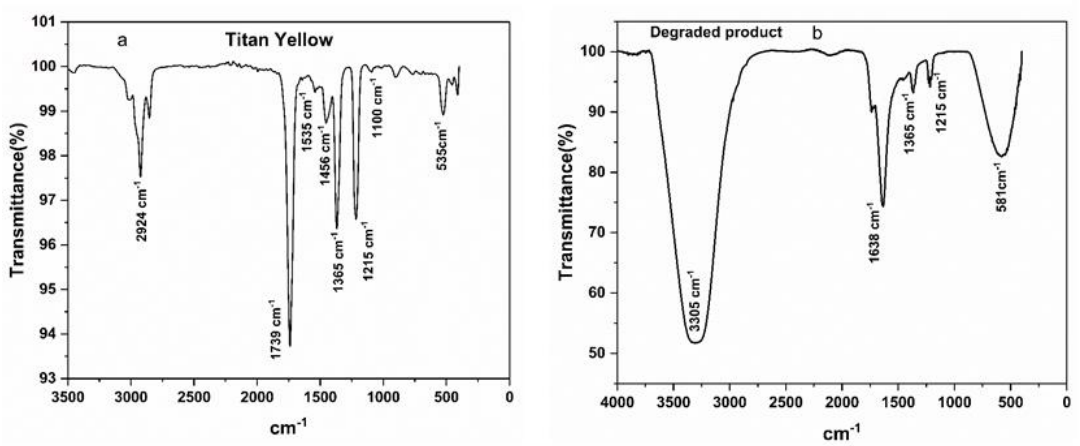

Fig.9 (a, b) FTIR spectra of TY dye and Degraded products

In this case, MoS_2, the used photocatalyst, has been examined for its reusability as shown in in figure (10). The impact of TY concentration was studied by varying the concentration from 5mg/L to 30mg/L, while keeping MoS_2 (40 mg/100 mL) constant are shown in figure (11). As the initial TY concentration was increased, the degradation percentage decreased. At initial TY concentrations of 5, 15, 30 mg/L, degradation efficiencies were 96%, 88%, 84%, respectively are shown in table1. The number of active sites in the photocatalyst decreases with increasing dye concentration. In high dye concentrations, the solution becomes more intensely colored and photons entering it have a shorter path length. This resulted in only a few photons reaching the catalyst surface which limits the production of hydroxyl radicals and superoxide radicals and decreases photodegradation (Nuengmatcha et al., 2023).

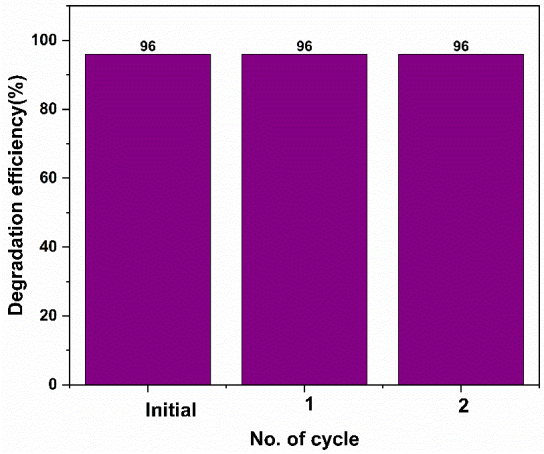

Fig.10 The degradation efficiency of TY dye w.r.t no. of cycles

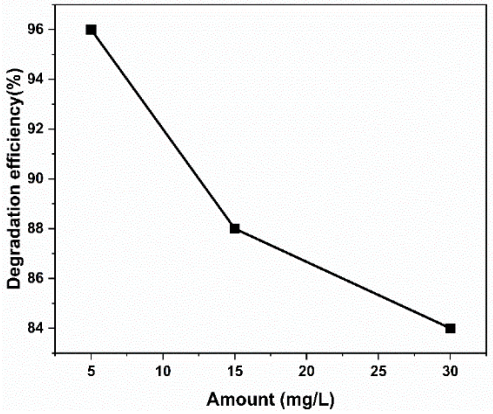

Fig.11 Effect of initial TY concentration at 40mg of MoS_2 photocatalyst

Table 1. Comparison of degradation efficiency with respect to concentration of dye and amount of catalyst used

Dye used	100ml, 5mg/L	100ml, 15 mg/L	100ml, 30 mg/L
Catalyst amount taken	40 mg	40 mg	40 mg
Efficiency (%)	96	88	84

Table 2. Overview of the photocatalytic degradation of MoS_2-based materials

Catalyst	Preparation technique	Irradiation source	Contaminant	Initial concentration (dye, catalyst)	Irradiation time (min)	Efficiency (%)	Ref.
TiO_2	Plant extract mediated synthesis of nano TiO_2	UV 125W	Titan yellow (TY)	10ppm,0.75g/l	120	95	(Hiremath et al., 2018)
Co NPs	Thermal decomposition	e mercury vapour lamp (100) W	Titan yellow (TY)	100mL(1.0 × 10-4 M), 0.0020g	40	51	(Chowdhury et al., 2020)
TiO_2-Fe_2O_3	Solution combustion method	mercury vapour lamp (125) W	Titan yellow (TY)	250 mL of 20ppm,60mg	60	92	(Kumar et al., 2020)
Zn_2TiO_4: Sm^{3+}	Solution combustion route	125 W mercury vapour lamp as source of UV light	Titan yellow (TY)	20 ppm of 250ml,60mg	60	80	(Girish et al., 2018)
SnO_2 decorated MoS_2	Hydro thermal	Visible 300 W Xe Lamp	MB	50 mL of 100 ppm of MB	120 minutes	58.5	(Rani et al., 2020)
MoS_2 nanosheet	Hydrothermal	Sunlight	TY	100ml(10mg/l),40 mg	12 minutes	96	Current work

Conclusion

In this research, MoS_2 nanosheet were synthesized and extensively examined for their structural and morphological characteristics. These produced nanosheet were then used for the photocatalytic degradation of TY dye. According to the results of the research, just 40mg of the catalyst was sufficient to degrade 96% of 100ml of dye solution (5mg/L) in under 12 minutes. The computed pseudo-kinetic rates at first order were 0.25 min^{-1}, demonstrating the exceptional effectiveness of the catalyst. The catalyst also showed remarkable reusability, with degrading efficiencies of 96% being maintained throughout the second and third cycles. These findings validate MoS_2 nanosheet potential as highly efficient catalysts for the degradation of TY dye under natural conditions. The ease, low cost, reusability, and tremendous performance of this procedure make it more suitable for industrial effluent treatment.

References

Agasti N (2021) Decontamination of heavy metal ions from water by composites prepared from waste. Current Research in Green and Sustainable Chemistry 4:100088. https://doi.org/10.1016/J.CRGSC.2021.100088

Alhammadi A, Alnaqbi W, Ashraf J, et al. (2020) Editors' Choice—Review—Conductive Forms of MoS2 and Their Applications in Energy Storage and Conversion. Journal of The Electrochemical Society 167:126517. https://doi.org/10.1149/1945-7111/ABB34B

Al-Tohamy R, Ali SS, Li F, et al. (2022) A critical review on the treatment of dye-containing wastewater: Ecotoxicological and health concerns of textile dyes and possible remediation approaches for environmental safety. Ecotoxicology and Environmental Safety 231:113160. https://doi.org/10.1016/J.ECOENV.2021.113160

Ashpak Shaikh A, Rajendra Patil M, Sonu Jagdale B, et al. (2023) Synthesis and characterization of Ag doped ZnO nanomaterial as an effective photocatalyst for photocatalytic degradation of Eriochrome Black T dye and antimicrobial agent. Inorganic Chemistry Communications 151:110570. https://doi.org/10.1016/J.INOCHE.2023.110570

Bhardwaj R, Jha R, Bhushan M, et al. (2020) Enhanced electrocatalytic activity of the solvothermally synthesized Mesoporous Rhombohedral nickel sulphide. Materials Science in Semiconductor Processing 118:105194. https://doi.org/10.1016/J.MSSP.2020.105194

Carolin CF, Kumar PS and Joshiba GJ (2021) Sustainable approach to decolourize methyl orange dye from aqueous solution using novel bacterial strain and its metabolites characterization. Clean

Technologies and Environmental Policy 23(1):173–181. https://doi.org/10.1007/S10098-020-01934-8/FIGURES/5

Chowdhury B, Pradhan SS, Das HS, et al. (2020) Visible Light Induced Photocatalytic Dye Degradation by Cobalt Oxide Nanoparticles. Fine Chemical Engineering :104–117. https://doi.org/10.37256/FCE.122020559

Dipti, Phogat P, Shreya, et al. (2023) Fabrication of tunable band gap carbon based zinc nanocomposites for enhanced capacitive behaviour. Physica Scripta 98(9). https://doi.org/10.1088/1402-4896/ACF07B

Dutta S, Adhikary S, Bhattacharya S, et al. (2024) Contamination of textile dyes in aquatic environment: Adverse impacts on aquatic ecosystem and human health, and its management using bioremediation. Journal of Environmental Management 353:120103. https://doi.org/10.1016/J.JENVMAN.2024.120103

Gautam S, Agrawal H, Thakur M, et al. (2020) Metal oxides and metal organic frameworks for the photocatalytic degradation: A review. Journal of Environmental Chemical Engineering 8(3):103726. https://doi.org/10.1016/J.JECE.2020.103726

Girish KM, Prashantha SC, Nagabhushana H, et al. (2018) Multi-functional Zn2TiO4:Sm3+ nanopowders: Excellent performance as an electrochemical sensor and an UV photocatalyst. Journal of Science: Advanced Materials and Devices 3(2):151–160. https://doi.org/10.1016/j.jsamd.2018.02.001

Hayashi T, Nakamura K, Suzuki T, et al. (2020) OH radical formation by the photocatalytic reduction reactions of H2O2 on the surface of plasmonic excited Au-TiO2 photocatalysts. Chemical Physics Letters 739:136958. https://doi.org/10.1016/J.CPLETT.2019.136958

Hiremath S, Antony Raj MAL, Chandra Prabha MN, et al. (2018) Tamarindus indica mediated biosynthesis of nano TiO2 and its application in photocatalytic degradation of Titan yellow. Journal of Environmental Chemical Engineering 6(6):7338–7346. https://doi.org/10.1016/j.jece.2018.08.052

Jaleel UC JR, Pinheiro D, et al. (2022) Architecture of visible-light induced Z-scheme MoS2/g-C3N4/ZnO ternary photocatalysts for malachite green dye degradation. Environmental research 214(Pt 1). https://doi.org/10.1016/J.ENVRES.2022.113742

Ji X, Bai Z, Luo F, et al. (2022) High-Performance Photodetectors Based on MoTe2-MoS2van der Waals Heterostructures. ACS Omega 7(12):10049–10055. https://doi.org/10.1021/ACSOMEGA.1C06009/ASSET/IMAGES/LARGE/AO1C06009_0005.JPEG

Kumar MRA, Abebe B, Nagaswarupa HP, et al. (2020) Enhanced photocatalytic and electrochemical performance of TiO2-Fe2O3 nanocomposite: Its applications in dye decolorization and as supercapacitors. Scientific Reports 10(1):1–15. https://doi.org/10.1038/s41598-020-58110-7

Kumar N, Bhadwal AS, Mizaikoff B, et al. (2019) Electrochemical detection and photocatalytic performance of MoS2/TiO2 nanocomposite against pharmaceutical contaminant: Paracetamol. Sensing and Bio-Sensing Research 24:100288. https://doi.org/10.1016/J.SBSR.2019.100288

Kumari H, Sonia, Suman, et al. (2023) A Review on Photocatalysis Used For Wastewater Treatment: Dye Degradation. Water, Air, & Soil Pollution 2023 234:6 234(6):1–46. https://doi.org/10.1007/S11270-023-06359-9

Lanjwani MF, Tuzen M, Khuhawar MY, et al. (2024) Trends in photocatalytic degradation of organic dye pollutants using nanoparticles: A review. Inorganic Chemistry Communications 159:111613. https://doi.org/10.1016/J.INOCHE.2023.111613

Lin J, Ye W, Xie M, et al. (2023) Environmental impacts and remediation of dye-containing wastewater. Nature Reviews Earth & Environment 2023 4:11 4(11):785–803. https://doi.org/10.1038/s43017-023-00489-8

Nayak D, Kumar A and Thangavel R (2023) Synthesis of MoS2 Nanoflowers for Photocatalytic Degradation of Organic Dyes. ACS Applied Nano Materials 6(20):19476–19490. https://doi.org/10.1021/ACSANM.3C04316

Nemiwal M, Zhang TC and Kumar D (2021) Recent progress in g-C3N4, TiO2 and ZnO based photocatalysts for dye degradation: Strategies to improve photocatalytic activity. Science of The Total Environment 767:144896. https://doi.org/10.1016/J.SCITOTENV.2020.144896

Nuengmatcha P, Kuyyogsuy A, Porrawatkul P, et al. (2023) Efficient degradation of dye pollutants in wastewater via photocatalysis using a magnetic zinc oxide/graphene/iron oxide-based catalyst. Water Science and Engineering 16(3):243–251. https://doi.org/10.1016/J.WSE.2023.01.004

Nur ASM, Sultana M, Mondal A, et al. (2022) A review on the development of elemental and codoped TiO2 photocatalysts for enhanced dye degradation under UV–vis irradiation. Journal of Water Process Engineering 47:102728. https://doi.org/10.1016/J.JWPE.2022.102728

Panchu SJ, Raju K, Swart HC, et al. (2021) Luminescent MoS2Quantum Dots with Tunable Operating Potential for Energy-Enhanced Aqueous Supercapacitors. ACS Omega 6(7):4542–4550.https://doi.org/10.1021/ACSOMEGA.0C02576/SUPPL_FILE/AO0C02576_SI_001.PDF

Pascariu P, Gherasim C and Airinei A (2023) Metal Oxide Nanostructures (MONs) as Photocatalysts for Ciprofloxacin Degradation. International Journal of Molecular Sciences 24(11). https://doi.org/10.3390/IJMS24119564

Rahman QI, Ali A, Ahmad N, et al. (2020) Synthesis and Characterization of CuO Rods for Enhanced Visible Light Driven Dye Degradation. Journal of Nanoscience and Nanotechnology 20(12):7716–7723. https://doi.org/10.1166/JNN.2020.18713

Rani A, Singh K, Patel AS, et al. (2020) Visible light driven photocatalysis of organic dyes using SnO2 decorated MoS2 nanocomposites. Chemical Physics Letters 738:136874. https://doi.org/10.1016/J.CPLETT.2019.136874

Sahoo D, Kumar B, Sinha J, et al. (2020) Cost effective liquid phase exfoliation of MoS2 nanosheets and photocatalytic activity for wastewater treatment enforced by visible light. Scientific Reports 2020 10:1 10(1):1–12. https://doi.org/10.1038/s41598-020-67683-2

Sahoo D, Shakya J, Ali N, et al. (2022) Edge Rich Ultrathin Layered MoS2Nanostructures for Superior Visible Light Photocatalytic Activity. Langmuir 38(4):1578–1588. https://doi.org/10.1021/ACS.LANGMUIR.1C03013/SUPPL_FILE/LA1C03013_SI_001.PDF

Shinde PH, Padwal Y, Waghadkar Y, et al. (2023) ZnS–MoS2 nano-heterostructure: efficient photocatalyst for dye removal under sunlight. Journal of Materials Science: Materials in Electronics 34(24):1–11. https://doi.org/10.1007/S10854-023-11105-2/FIGURES/10

Singh J, Rishikesh, Kumar S et al. (2020) Synthesis of 3D-MoS2 nanoflowers with tunable surface area for the application in photocatalysis and SERS based sensing. Journal of Alloys and Compounds 849:156502. https://doi.org/10.1016/J.JALLCOM.2020.156502

Sultana M, Mondal A, Islam S, et al. (2023) Strategic development of metal doped TiO2 photocatalysts for enhanced dye degradation activity under UV–Vis irradiation: A review. Current Research in Green and Sustainable Chemistry 7:100383. https://doi.org/10.1016/J.CRGSC.2023.100383

Yadav S, Shakya K, Gupta A, et al. (2022) A review on degradation of organic dyes by using metal oxide semiconductors. Environmental Science and Pollution Research 2022 30:28 30(28):71912–71932. https://doi.org/10.1007/S11356-022-20818-6

Yuan Y, Guo R tang, Hong L fei, et al. (2021) Recent advances and perspectives of MoS2-based materials for photocatalytic dyes degradation: A review. Colloids and Surfaces A: Physicochemical and Engineering Aspects 611. https://doi.org/10.1016/J.COLSURFA.2020.125836

Author Contributions
AK, M, RB, DDY, A and RJ conceived the concept, wrote and approved the manuscript.

Acknowledgements
The authors are grateful for financial assistance to Netaji Subhas University of Technology (NSUT) and University Grant Commission (UGC).

Funding
Not applicable.

Availability of data and materials
Not applicable.

Competing interest
The authors declare no competing interests.

Ethics approval
Not applicable.

Citation: Kumar A, Manisha, Bhardwaj R, Yadav DD, Anju and Jha R (2024) One Pot Synthesized 2H - MoS_2 as Efficient Photocatalyst for Degradation of Titan Yellow Dye under Solar Light Illumination. Environ Sci Arch 3(2): 103-115.